

# Identification of a Control Oriented Nonlinear Dynamic USV Model

Kenneth R. Muske and Hashem Ashrafiuon

Center for Nonlinear Dynamics and Control, Villanova University, Villanova, PA 19085

Geoffrey Haas and Ryan McCloskey

Department of Mechanical Engineering, Villanova University, Villanova, PA 19085

Timothy Flynn

Department of Electrical and Computer Engineering, Villanova University, Villanova, PA 19085

## Abstract

The identification of the parameters in a three degree of freedom nonlinear dynamic surface vessel model using drag test data in each of the axes of motion is presented in this work. Parameter estimates based on the use of terminal velocity measurements and on the use of dynamic position measurements are determined and compared. The identification procedure is carried out on an experimental model boat which is used as the basis for comparison.

## 1. Introduction

The design of trajectory tracking and guidance control systems for unmanned surface vehicles (USV) depends on an accurate control oriented model of the vessel dynamics. Models of varying complexity have been proposed to describe the kinematics and hydrodynamics of surface vessel motion [1]. A uniform requirement for the application of these models is the identification of the model parameters which are typically vessel dependent. Various techniques to obtain model parameter estimates from experimental or sea trial data, such as the extended Kalman filter [2],[3], simulated annealing [4], maximum likelihood [5], and adaptive estimation [6], have been proposed.

The motivation for this work is the supervisory control and coordination of a USV fleet to perform surveillance, search and rescue, and similar functions. The dynamic USV models are used to both design the local autopilot controls for each USV and to describe the dynamics for trajectory planning and optimization by the supervisory controller. Because the proposed applica-

tion must address a USV fleet with the potential for a large number of different vessels, model parameter identification can represent a significant experimental effort. The advantage of this application, however, is that the USV fleet will typically consist of small vessels that can be easily towed using standard shore-based towing equipment. The use of towing tests and maneuvering experiments for small vessels is discussed in [7]. Designing drag tests in which the vessel dynamics, and the associated model parameters, are isolated to a single axis of motion greatly simplifies parameter identification. This work presents an experimental demonstration of this approach.

## 2. Experimental USV System

All experiments are performed using a 0.51m long 1.614kg radio-controlled, battery-powered model boat in a 6ft x 8ft indoor pool. Two DC electric motors, each mounted to a separate propeller shaft, provide the propulsion power. The propellers are located 0.07m apart to also provide steering torque. There is no rudder on the model boat. A joystick controls the boat using a wireless receiver. It has been modified so that control signals can be transmitted from a dSpace board connected to a control computer. A digital black and white camera mounted 6ft above the center of the pool is used to provide feedback measurements of the boat position in real time. The camera captures an image of the entire pool area at a rate of 30 frames/sec. Two infrared LED's of different intensities are installed at the front and rear of the centerline of the boat. The two resulting infrared images are detected in the

image captured by the camera and used to determine the position and the orientation of the boat. Navigational GPS and compass systems provide these measurements on the actual USV.

Because the camera image is distorted, calibration is necessary to translate pixel location in the camera frame to physical location in the pool. Calibration is carried out by placing a board with a series of LED's installed at regular intervals on the top of the pool at known locations and recording the camera image pixel matrix. The camera image pixel matrix locations of all LED's and their corresponding physical positions are shown in Figure 1. Two dimensional cubic interpolation functions are used to fit the physical location to the image matrix. The position estimate for the image matrix in Figure 1 using these interpolation functions is shown in Figure 2. These interpolation functions are used to determine the location of the two infrared LED's attached to the model boat.

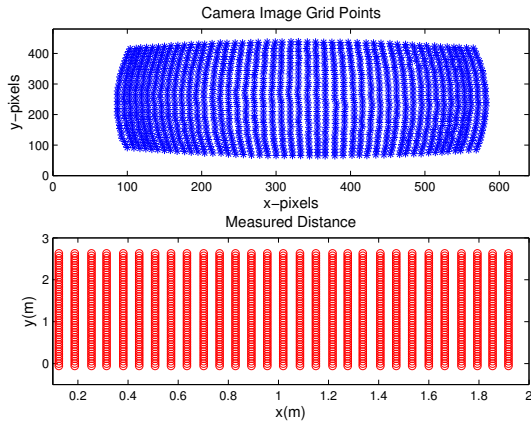


Figure 1: Camera calibration points and image.

### 3. Planar USV Dynamic Model

The three degree of freedom surface vessel model presented in [1] is used to describe the motion of the USV. This planar model neglects heave, pitch, and roll dynamics. The resulting equations of motion in body-fixed coordinates are

$$m_{11}\dot{v}_x - m_{22}v_y\omega_z + d_1v_x^{\alpha_1} = f_p \quad (1)$$

$$m_{22}\dot{v}_y + m_{11}v_x\omega_z + d_2v_y^{\alpha_2} = 0 \quad (2)$$

$$m_{33}\dot{\omega}_z + m_{22-11}v_xv_y + d_3\text{sgn}(\omega_z)|\omega_z|^{\alpha_3} = T_s \quad (3)$$

where  $v_i$  are the linear velocities of the vessel,  $\omega_z$  is the rotational velocity,  $m_{ii}$  are the mass

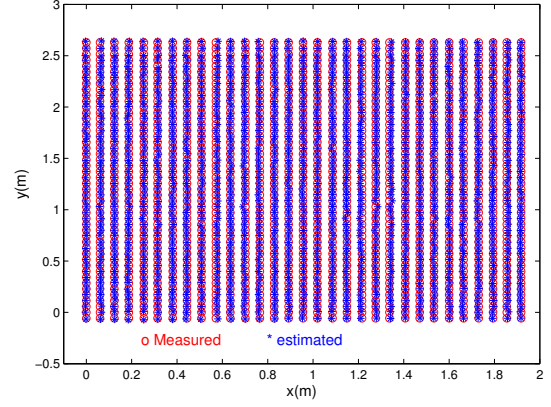


Figure 2: Calibrated camera image vs. position.

parameters,  $d_i, \alpha_i$  are the nonlinear damping coefficients, and only forward motion is considered in this model. The mass and damping terms are assumed to be constant and a power law velocity relationship is used to describe the hydraulic drag forces and torque. The propulsion force  $f_p$  and steering torque  $T_s$  are functions of the two surge control forces from each propeller

$$f_p = f_1 + f_2 \quad (4)$$

$$T_s = B(f_1 - f_2)/2 \quad (5)$$

where  $f_1$  is produced by the first motor and  $f_2$  is produced by the second motor. The  $m_{ii}$  mass parameters include added mass contributions that represent hydraulic pressure forces and torque due to forced harmonic motion of the vessel which are proportional to acceleration. Using the estimate of the added mass terms presented in [1] for the experimental model boat results in

$$m_{11} \approx m + 0.05m = 1.695 \text{ kg} \quad (6)$$

$$m_{22} \approx m + 0.5(\rho\pi D^2L) = 1.865 \text{ kg} \quad (7)$$

$$m_{33} \approx \frac{m(L^2 + W^2) + \frac{1}{2}(0.1mB^2 + \rho\pi D^2L^3)}{12} \quad (8)$$

$$= 0.0275 \text{ kgm}^2$$

where  $m = 1.614\text{kg}$  is the actual mass,  $L = 0.4\text{m}$  is the effective length,  $W = 0.14\text{m}$  is the width,  $D = 0.02\text{m}$  is the mean submerged depth,  $B = 0.07\text{m}$  is the distance between the propellers, and  $\rho$  is the density of water. The vessel position in the inertial reference coordinates  $z = [x, y, \theta]^T$  which represent the  $x$ - $y$  location of the center of

mass and the orientation angle of the vessel are

$$\dot{x} = v_x \cos \theta - v_y \sin \theta \quad (9)$$

$$\dot{y} = v_x \sin \theta + v_y \cos \theta \quad (10)$$

$$\dot{\theta} = \omega \quad (11)$$

Figure 3 presents a schematic of the model USV.

#### 4. Parameter Estimation

The USV model in Eqs. 1– 3 contains nine parameters, three mass parameters and six nonlinear damping coefficients, that must be determined from experimental vessel data. By restricting the USV motion to a single direction along the horizontal ( $x$ ), lateral ( $y$ ), and rotational ( $z$ ) axes in these experiments, the cross terms in Eqs. 1– 3 are eliminated resulting in the following relationships for each axis

$$m_{11}\dot{v}_x + d_1v_x^{\alpha_1} = f_x, v_y = \omega_z = 0 \quad (12)$$

$$m_{22}\dot{v}_y + d_2v_y^{\alpha_2} = f_y, v_x = \omega_z = 0 \quad (13)$$

$$m_{33}\dot{\omega}_z + d_3\text{sgn}(\omega_z)|\omega_z|^{\alpha_3} = T_z, v_x = v_y = 0 \quad (14)$$

where  $f_x$  is the horizontal force providing motion only in the  $x$  direction,  $f_y$  is the lateral force providing motion only in the  $y$  direction, and  $T_z$  is the rotational torque providing only rotational motion. The mass and damping terms corresponding to each axis can be estimated independently using drag experiments conducted along the individual axes. The result is a simpler estimation problem with fewer parameters.

##### 4.1. Terminal Velocity Experiments

An estimate of the nonlinear damping coefficients  $d_i$ ,  $\alpha_i$  can be obtained using the terminal velocity from experimental drag data in each of the three axes of motion. The steady-state relationships for the  $x$ ,  $y$ , and  $z$  directions are

$$d_1v_x^{\alpha_1} = f_x, d_2v_y^{\alpha_2} = f_y, d_3\omega_z^{\alpha_3} = T_z \quad (15)$$

where  $\omega_z > 0$ . A power law curve fit of the constant force and velocity experimental data can be used to determine the damping coefficients. Velocity may either be measured directly or estimated from the slope of a plot of position versus time. The mass parameters, however, can not be estimated with this approach using only the terminal velocity. They must be approximated using the relationships presented in Eqs. 6–8.

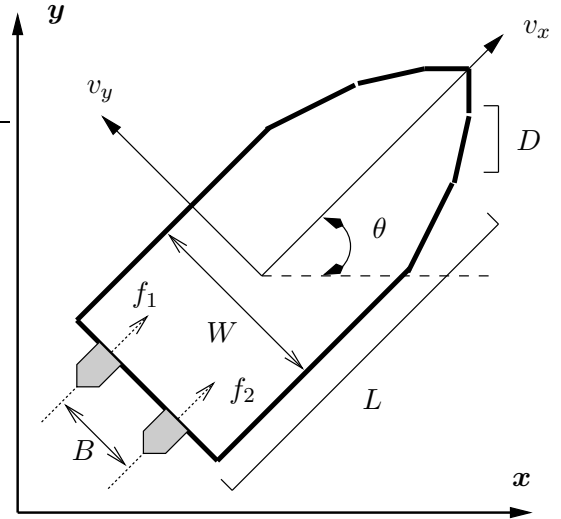


Figure 3: Planar USV model schematic.

##### 4.2. Dynamic Position Experiments

For experimental data in which information concerning the measurement variance for each type of measurement is available *a priori*, the maximum likelihood model parameter estimate can be obtained by the solution of a weighted least squares problem [8]. The least squares problem in this work is the minimization of the weighted sum of the squared error between the model predicted and measured USV position

$$\min_{\{m_{ii}, d_i, \alpha_i\}} \sum_{k=1}^N \sum_{j=1}^{J_k} \left\| \mathbf{z}_{j,k}^m - \mathbf{z}_{j,k}^p \right\|_{\mathbf{Q}^{-1}}^2 \quad (16)$$

where  $k$  refers to the experiment number,  $J_k$  is the number of data samples taken for experiment  $k$ ,  $\mathbf{z}_{j,k}^m$  is the measured position vector for the  $j$ th sample of the  $k$ th experiment,  $\mathbf{z}_{j,k}^p$  is the model predicted position vector for the  $j$ th sample of the  $k$ th experiment, and  $\mathbf{Q}$  is the measurement covariance matrix. The measured boat positions are obtained from dynamic drag experiments in each axis of motion and the model predicted positions are determined from the solution of the corresponding ODE in Eqs. 12– 14.

A linear approximation to the confidence intervals for the model parameters is obtained by assuming that the model can be represented by a series of linear functions in a neighborhood of

the estimated parameter values  $\hat{\mathbf{p}}$

$$z_{i,j,k}(\mathbf{p}) \approx z_{i,j,k}(\hat{\mathbf{p}}) + \Delta z_{i,j,k}(\mathbf{p} - \hat{\mathbf{p}}) \quad (17)$$

$$\Delta z_{i,j,k} = \left. \frac{\partial z_{i,j,k}}{\partial \mathbf{p}} \right|_{\mathbf{p}=\hat{\mathbf{p}}}$$

where  $\mathbf{p}$  is the vector of model parameters,  $z_{i,j,k}$  is the model predicted position for the  $i$ th axis of the  $j$ th sample of the  $k$ th experiment, and  $\Delta z_{i,j,k}$  is the  $1 \times 3$  sensitivity vector. Assuming normally distributed prediction errors, the region containing  $100(1 - \alpha)$  percent of the probability expressed by the linearized parameter posterior distribution is represented by [9]

$$\chi_p^2(\alpha) = (\mathbf{p} - \hat{\mathbf{p}})^T \mathbf{V}^{-1} (\mathbf{p} - \hat{\mathbf{p}}) \quad (18)$$

$$\mathbf{V}^{-1} = \sum_{i=1}^n \sigma_i^{-2} \sum_{k=1}^N \sum_{j=1}^{J_k} \Delta z_{i,j,k}^T \Delta z_{i,j,k}$$

where  $\chi_p^2(\alpha)$  is the value of the chi-square distribution for  $p$  degrees of freedom evaluated at  $\alpha$ ,  $p$  is the number of estimated parameters,  $\mathbf{V}$  is the covariance matrix of the linearized parameter posterior distribution,  $n = 3$  is the dimension of  $\mathbf{z}$ , and  $\sigma_i^2$  is the measurement variance for the  $i$ th position. The hyperbox in the parameter space that circumscribes this ellipsoidal confidence region is determined as follows [10]

$$p_i \approx \hat{p}_i \pm \sqrt{\mathbf{V}(i,i) \chi_p^2(\alpha)} \quad (19)$$

in which  $p_i$  is the  $i$ th component of the parameter vector,  $\mathbf{V}(i,i)$  is the  $i$ th diagonal element of the parameter covariance matrix of the linearized distribution, and  $\alpha = 0.05$  is the level of significance for a 95% confidence interval.

## 5. Identification Experimental Results

Experimental drag tests using a series of constant forces in each of the axes of motion was carried out on the model boat. Terminal velocities for each experiment were estimated from the slope of a position versus time plot after the boat reached a constant velocity. An estimate of the variance of the position measurements was obtained by pooling the variance of the difference between the linear velocity fit and the measured position data at constant velocity for each experiment.

$$\sigma_x^2 = 9.21 \times 10^{-5}, \quad \sigma_y^2 = 4.75 \times 10^{-4}, \quad \sigma_\theta^2 = 0.501$$

The differences are largely due to the relative increase in difficulty in keeping the boat straight during the lateral drag and the center of mass fixed during the rotational drag experiments. The nine parameter estimates based on the terminal velocity identification and dynamic position identification are presented in Table 1 where the mass terms for the terminal velocity identification were determined using Eqs. 6–8.

**Table 1:** Estimated model parameters.

<i>Parameter</i>	<i>Terminal</i>	<i>Dynamic</i>
$m_{11}$	1.695	$1.96 \pm 0.019$
$d_1$	2.72	$2.44 \pm 0.023$
$\alpha_1$	1.68	$1.51 \pm 0.0075$
$m_{22}$	1.865	$2.40 \pm 0.12$
$d_2$	13.4	$13.0 \pm 0.30$
$\alpha_2$	1.79	$1.75 \pm 0.013$
$m_{33}$	0.0275	$0.0430 \pm 0.0068$
$d_3$	0.0566	$0.0564 \pm 0.00085$
$\alpha_3$	1.58	$1.59 \pm 0.0285$

The dynamic position identification results in a significant increase in the mass terms and a reduction in the horizontal and lateral drag force parameters. The power law fits for the nonlinear damping coefficients from both the terminal velocity and dynamic position identification are presented in Figures 4–6 along with the experimental terminal velocity values for the horizontal, lateral, and rotational drag experiments.

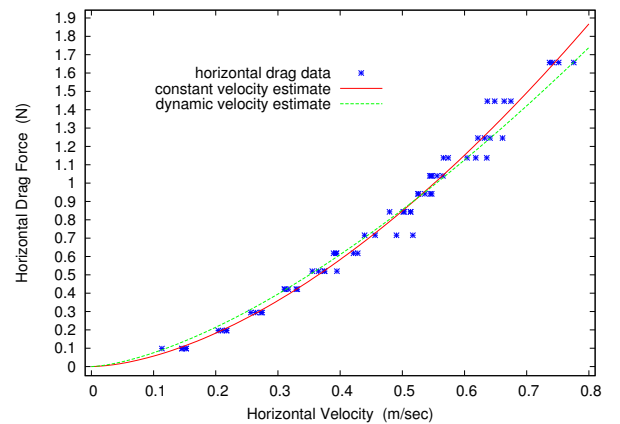


**Figure 4:** Horizontal drag force velocities.

Figure 7 presents an example horizontal drag experiment with the terminal velocity linear fit, terminal velocity parameter identification, and

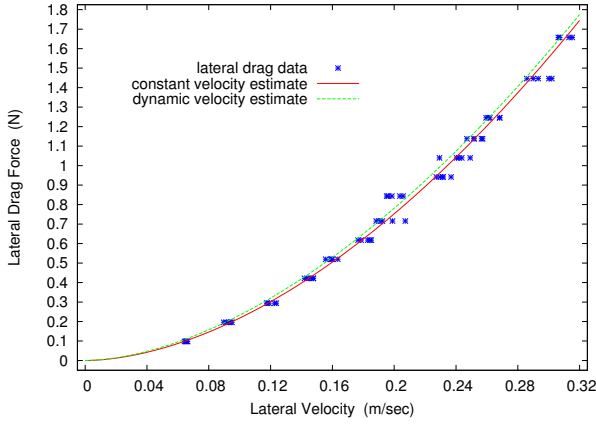


Figure 5: Lateral drag force velocities.

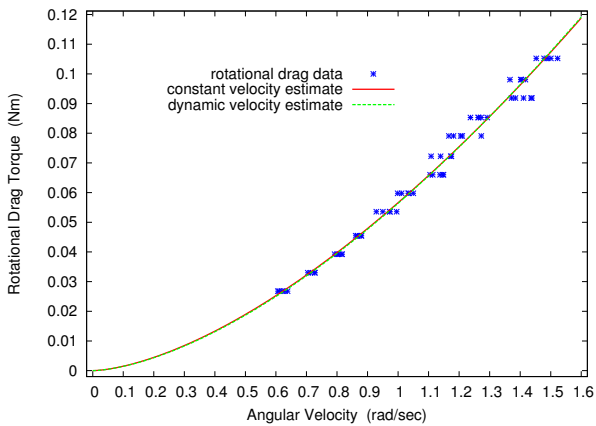


Figure 6: Rotational drag torque velocities.

dynamic position parameter identification model predictions. The increased mass term from dynamic position identification provides a much better fit to the initial motion while the terminal velocity predictions are essentially the same.

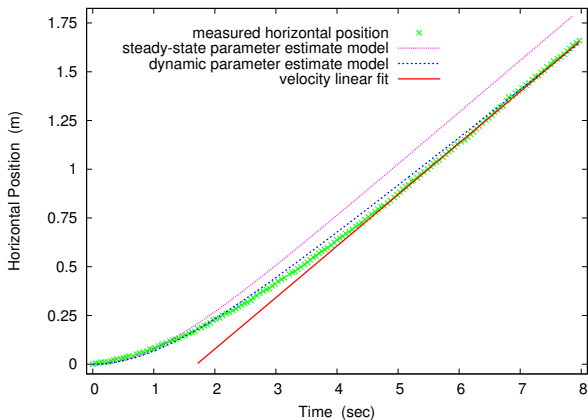


Figure 7: Example horizontal drag experiment.

## 6. Propeller Force Model

Because an accurate model of the motor and propeller dynamics is not available, an empirical relationship between the propeller force and motor input voltage is identified. A series of constant voltages were applied to both motors to produce horizontal motion. The corresponding propulsion force was determined by minimizing the least squares objective in Eq. 16 assuming constant and equal applied propeller forces  $f_1 = f_2 = f_p/2$ . The following quadratic relationships for applied motor voltages larger than 0.2V in the positive direction and less than -0.3V in the negative direction are shown in Figure 8.

$$V_i = \begin{cases} 5.04f_i^2 - 1.67f_i + 0.344, & f_i > 0 \\ -49.1f_i^2 - 1.43f_i - 0.299, & f_i < 0 \end{cases} \quad (20)$$

The dead band of the motors between -0.3V and 0.2V is indicated by the green box in Figure 8. Although the motors are not perfectly balanced, the force-voltage relations are assumed identical.

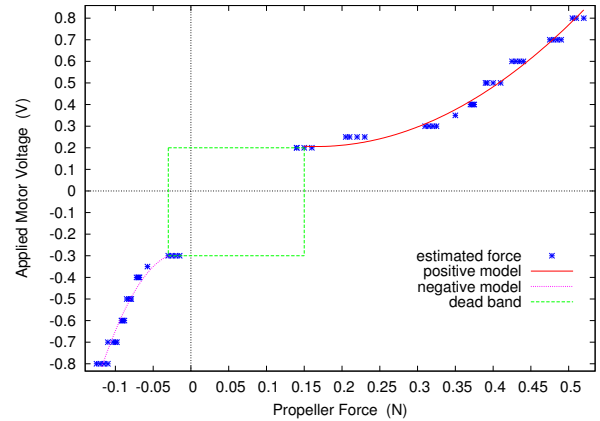
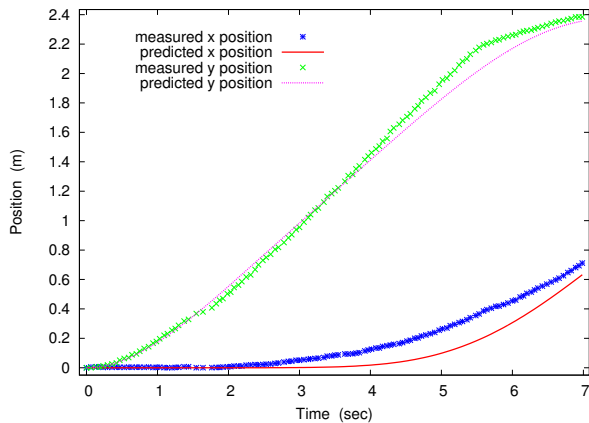


Figure 8: Propeller force models.

## 7. Model Verification

The model parameters were validated against powered experimental data sets that were not used in the motor calibration. In these experiments, a constant voltage is initially applied to both motors with the boat at rest. After a short time period, a step change is made to the voltage one of the motors to produce a steering torque on the boat. Figure 9 presents the experimental and model predicted  $x$  and  $y$  coordinate trajectories for one of these experiments in which a voltage of 0.6V was applied to both motors for a period

of 2sec after which a step change to 0.3V was applied to the second motor producing a turning moment of approximately  $4.2 \times 10^{-3}$ Nm. A phase plot is presented in Figure 10. As shown in these figures, the model matches the data reasonably well except for a slight over prediction of the turning radius. It is also unable to account for the drift in the  $x$  coordinate. Because the motors are not perfectly balanced and there are unmeasured disturbances in the system, some drift in the experimental data is to be expected.



**Figure 9:** Model predicted  $x$  and  $y$  trajectory.

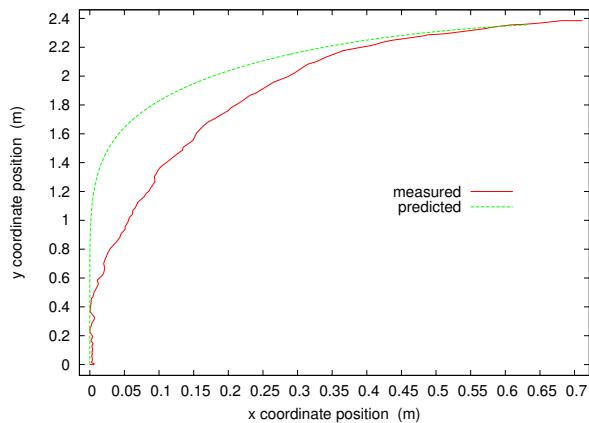


**Figure 10:** Model predicted phase plot.

## 8. Conclusions

The identification of USV model parameters using only drag tests that isolate the motion along the individual axes is presented in this work. One of the major advantages to this identification strategy is that the model parameters corresponding to each axis can be estimated indepen-

dently which requires less data for a reliable estimate. Experimental results using the model boat indicate that the procedure produces parameter estimates that are able to predict powered experimental data sets not used in the identification with reasonable accuracy.

## Acknowledgment

Support for this work from the Office of Naval Research under ONR grant N00014-04-1-0642 and the Center for Nonlinear Dynamics and Control (CENDAC) is gratefully acknowledged.

## References

- [1] T. Fossen. *Guidance and Control of Ocean Vehicles*. Wiley, New York, 1994.
- [2] T. Fossen, S. Sagatun, and A. Sorensen. Identification of dynamically positioned ships. *Contr. Eng. Prac.*, 4:369–376, 1996.
- [3] H. Yoon and K. Rhee. Identification of hydrodynamic coefficients in ship maneuvering. *Ocean Eng.*, 30(18):2379–2404, 2003.
- [4] A. Tiano and M. Blanke. Multivariable identification of ship steering and roll motions. *Trans. Inst. Meas. Contr.*, 19(2):63–77, 1997.
- [5] S. Dudnik. Identification by maximum likelihood method in modeling of ship movement. *Eng. Sim.*, 12(4):658–652, 1995.
- [6] M. Casado, R. Ferreiro, and F. Velasco. Identification of nonlinear ship model parameters. *J. Ship Res.*, 51(2):174–181, 2007.
- [7] R. Skjetne, O. Smogeli, and T. Fossen. A nonlinear ship maneuvering model: identification and adaptive control with experiments for a model ship. *Mod. Ident. Contr.*, 25(1):3–27, 2004.
- [8] G. Box and G. Tiao. *Bayesian Inference in Statistical Analysis*. Addison–Wesley, Reading, Mass., 1973.
- [9] Y. Bard. *Nonlinear Parameter Estimation*. Academic Press, New York, 1974.
- [10] V. Fedorov. *Theory of Optimal Experiments*. Academic Press, New York, 1972.